Supplement of Atmos. Chem. Phys., 21, 10065–10080, 2021
https://doi.org/10.5194/acp-21-10065-2021-supplement

Atmospheric Chemistry and Physics
Open Access
EGU

Supplement of

Quantitative assessment of changes in surface particulate matter concentrations and precursor emissions over China during the COVID-19 pandemic and their implications for Chinese economic activity

Hyun Cheol Kim et al.

Correspondence to: Hyuncheol Kim (hyun.kim@noaa.gov) and Soontae Kim (soontaekim@ajou.ac.kr)

Table S1 Responses of surface $PM_{2.5}$ concentration for emission reduction sensitivity tests. Baseline model was simulated using CMAQ with CREATE emission inventory for 2016. Changes of surface $PM_{2.5}$ concentrations (and percentages) from the baseline simulation are shown for 1) all emission 50% reduction, 2) SOx and NOx emission 35% reduction, 3) NOx emission 35% reduction, 4) SOx emission 35% reduction, and 5) NH_3 emission 35% reduction. BTH denotes for Beijing-Tianjin-Hebei region, and YRD&SD denotes Yangtze River Delta and Shandong region.

	Base Model	All Emission -50%	SOx&NOx -35%	NOx -35%	SOx -35%	NH3 -35%
China	36.9 μg/m^3	-18.9 μg/m^3 (-51 %)	-4.1 μg/m^3 (-11 %)	-2.9 μg/m^3 (-8 %)	-1.2 μg/m^3 (-3 %)	-3.3 μg/m^3 (-9 %)
BTH	53.4 μg/m^3	-26.8 μg/m^3 (-50 %)	-3.7 μg/m^3 (-7 %)	-2.2 μg/m^3 (-4 %)	-1.5 μg/m^3 (-3 %)	-4.1 μg/m^3 (-8 %)
YRD&SD	41.3 μg/m^3	-21.2 μg/m^3 (-51 %)	-4.4 μg/m^3 (-11 %)	-3.1 μg/m^3 (-8 %)	-1.3 μg/m^3 (-3 %)	-4.2 μg/m^3 (-10 %)

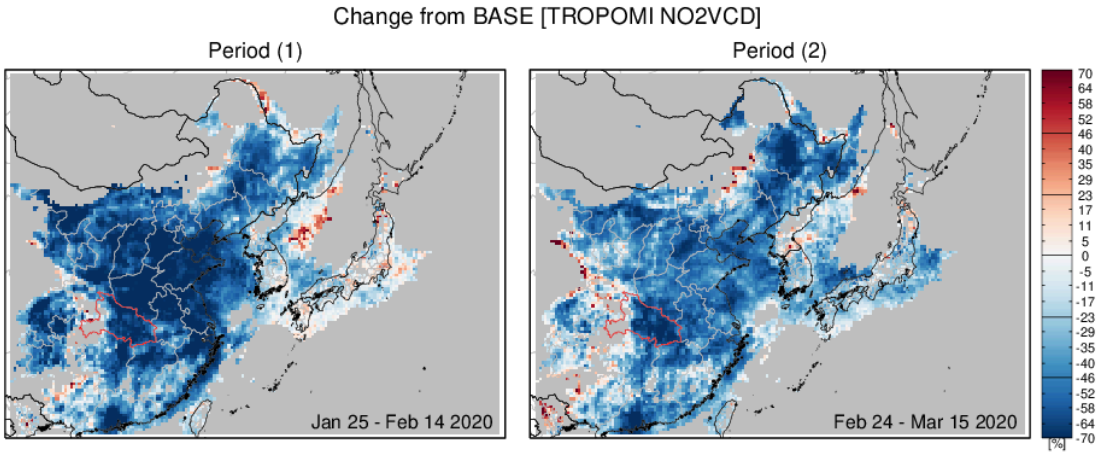

Figure S1 Spatial distribution of the change in TROPOMI NO_2 vertical column densities from the base period (Figure 1) during the maximum impact period (January 25 – February 14, 2020) and the recovery period (February 24 – March 15, 2020). Hubei province is marked in red. Areas with NO_2 column density less than 1x1015 mole/cm2 in the base period were marked in gray.

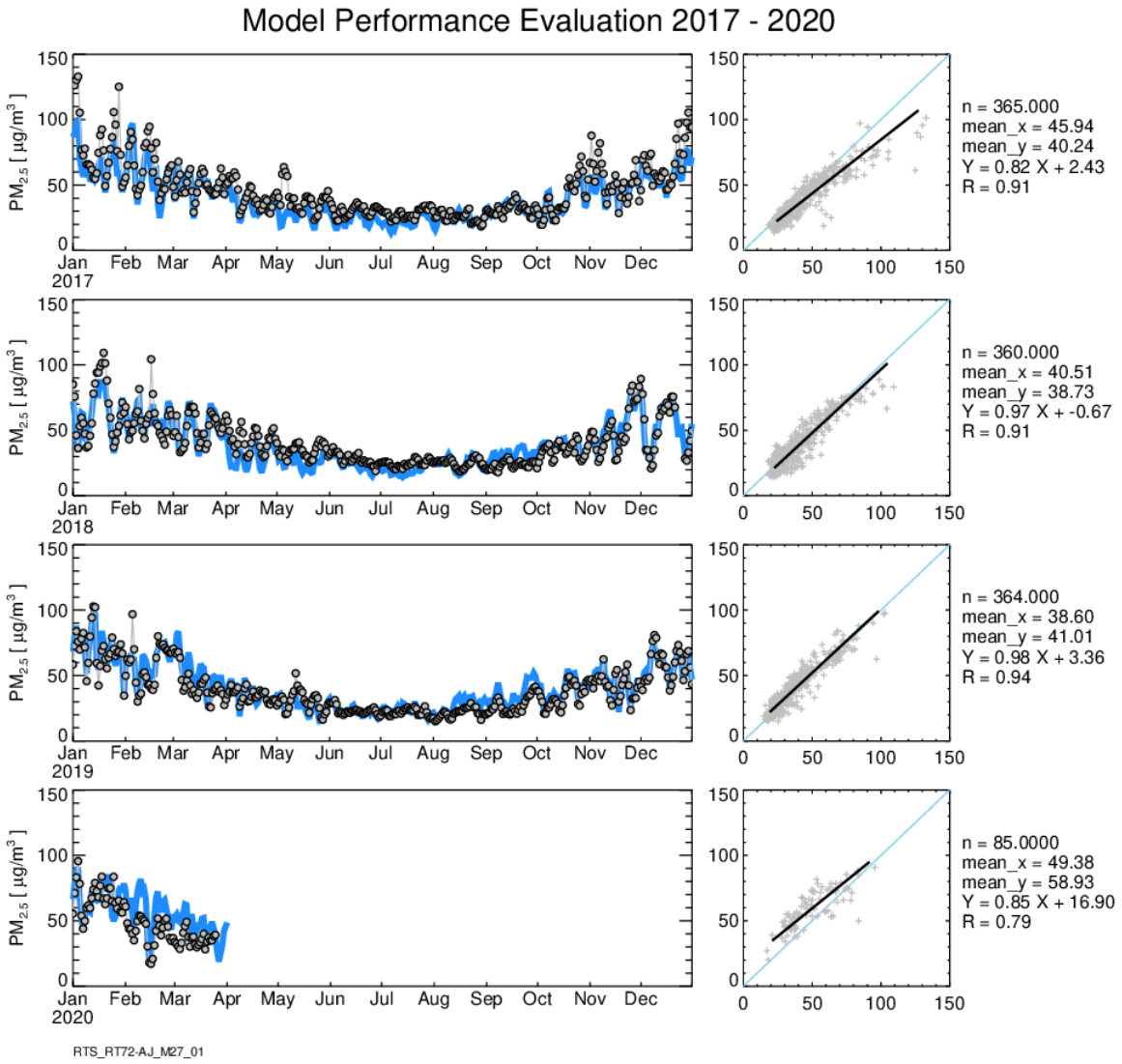

35

Figure S2 Time series comparisons of model and surface observations for $PM_{2.5}$, NO_2, and SO_2.

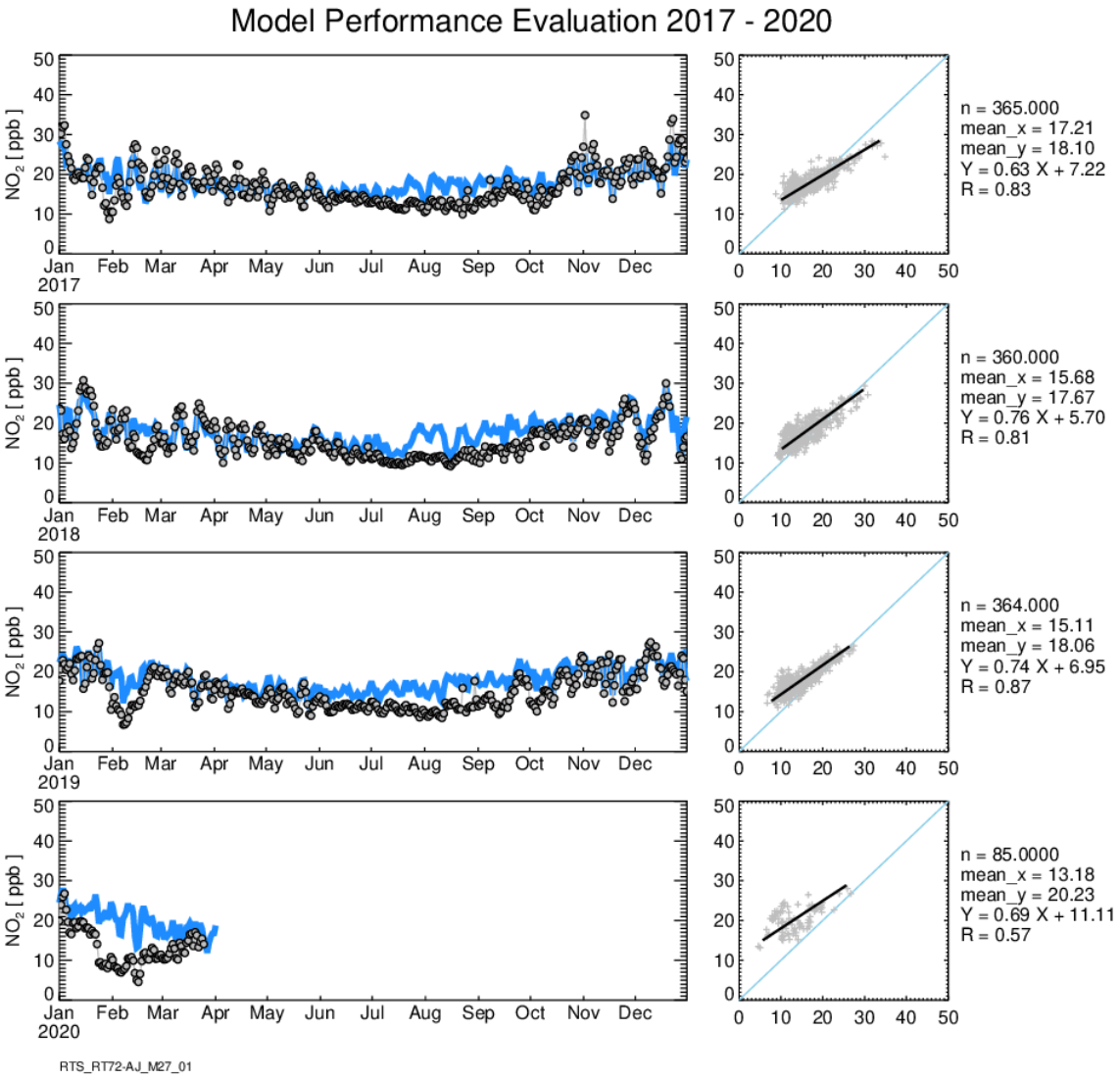

Figure S2. Continued

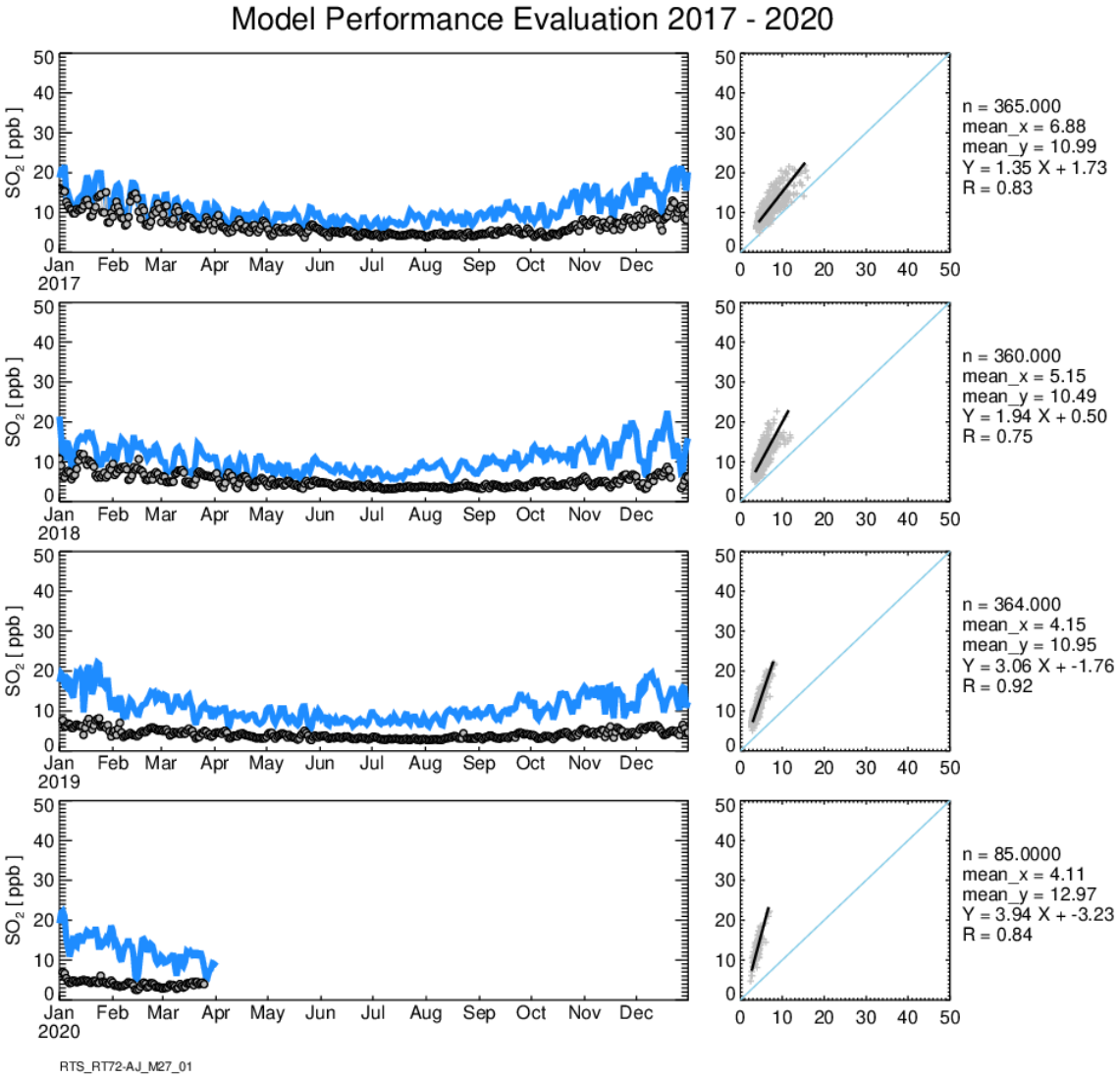

Figure S2. Continued.

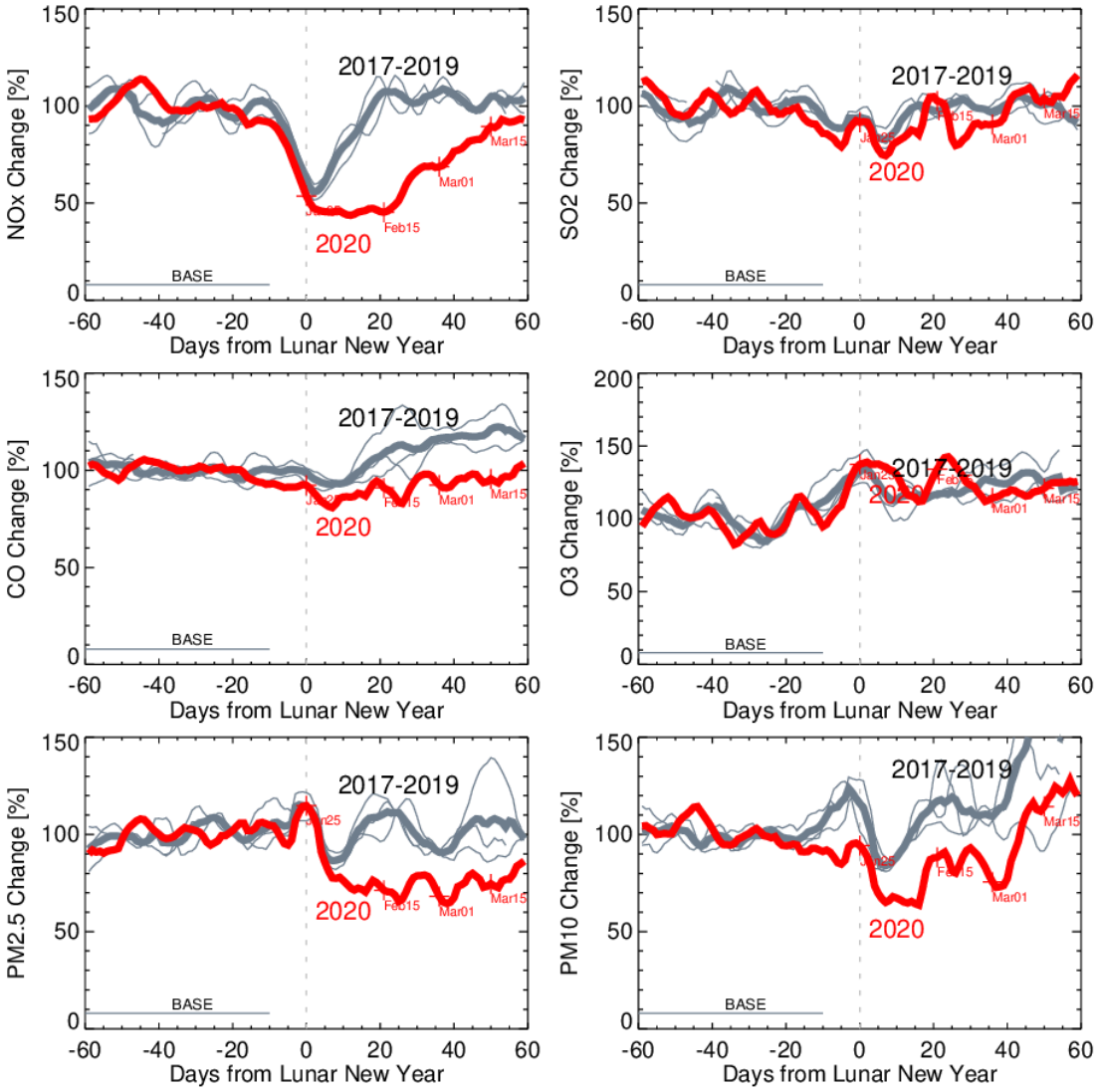

45 **Figure S3 Time series of estimated emissions changes for NO_2, SO_2, CO, O_3, $PM_{2.5}$, and PM_{10} using surface monitors across China. The gray lines indicate 2017–2019 variations with their average in the thick gray line, whereas the red line indicates the 2020 variation. BASE is used as the pre-LNY period, and time series was calculated as relative changes from the average of the base period.**

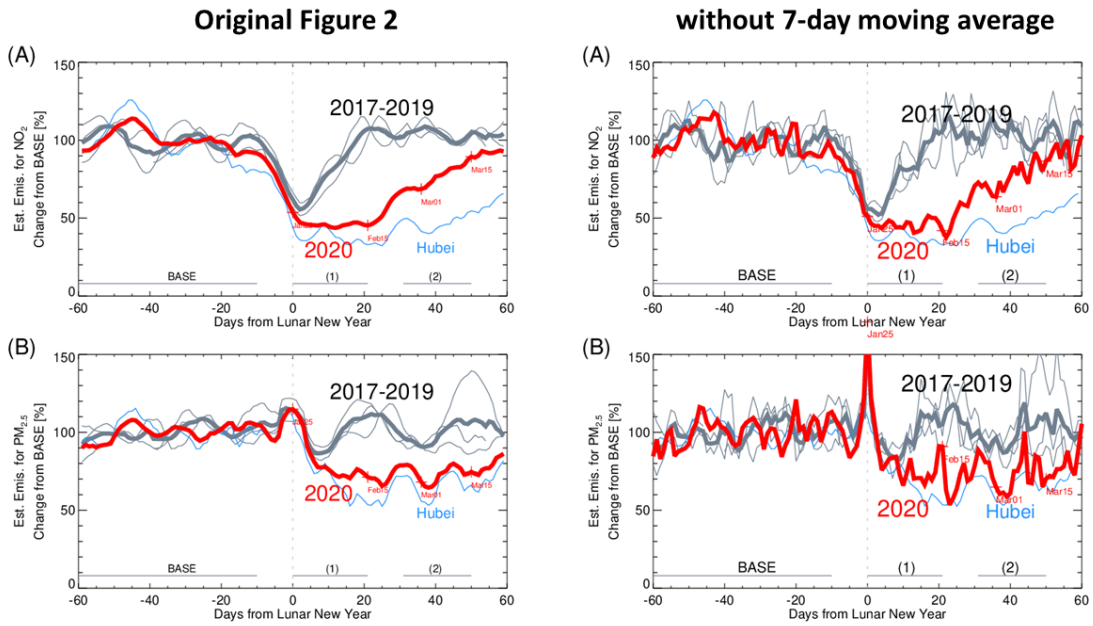

Figure S4 Comparison of the original time series by removing meteorological, weekly, yearly and the LNY signals (left) and the one without seven-day moving average (right). The seven-day moving average filtering is required to avoid unfair comparisons between different weekdays after the LNY alignment.

The seven-day moving average process was applied to remove unfair comparisons by comparing different days of the week. Since we applied an alignment to center the LNY, daily time series comparisons were performed for different weekdays in different years because LNY days were assigned to different weekdays. While the time series without seven-day moving average processing is a little noisier due to the unfair comparison between different weekdays, we do not see significant differences between the two plots. Therefore, our conclusions based on the results of this time-series analysis are valid irrespective of the use of seven-day moving-average processing.

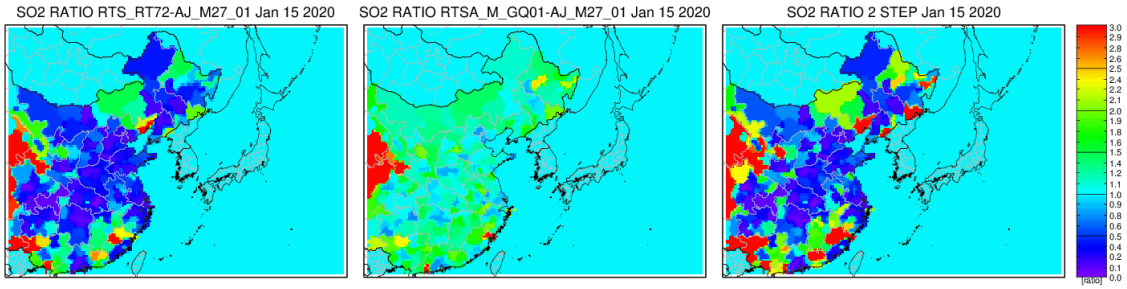

65 **Figure S5 Spatial distribution of SO_2 emission adjustment factors for 1-step adjustment (left), and β values (middle), and 2-step adjustment factors (right).**

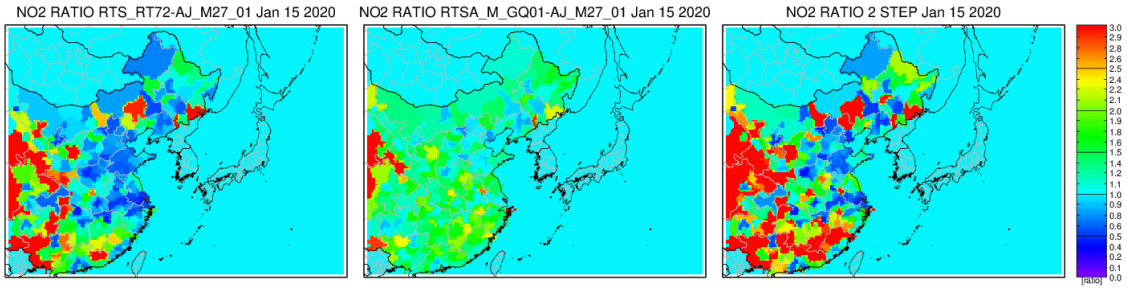

Figure S6 Spatial distribution of NO_2 emission adjustment factors for 1-step adjustment (left), and β values (middle), and 2-step adjustment factors (right).

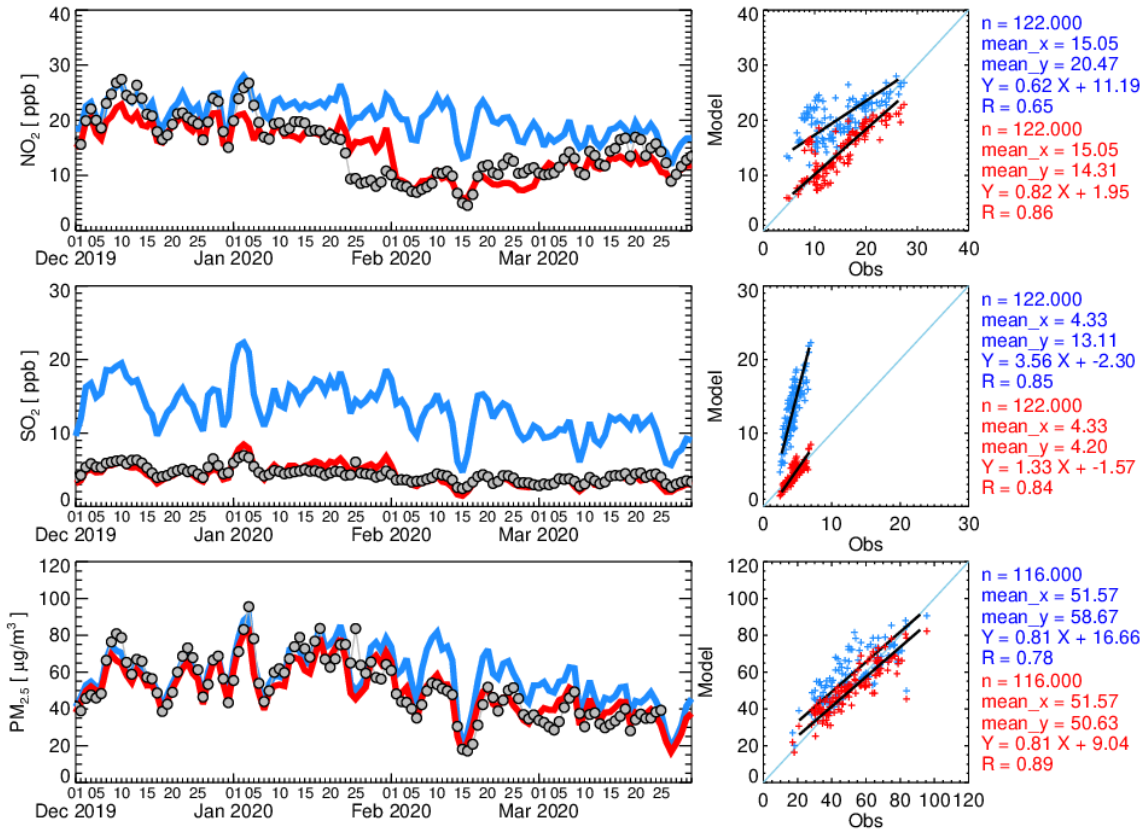

75

Figure S7 Time series of surface concentrations of NO_2, SO_2 and $PM_{2.5}$ for the baseline simulation (blue) and adjusted-emission simulations (red). Monthly emission adjustment factors were used with a fixed emission-to-concentration conversion factor (i.e. β=1).

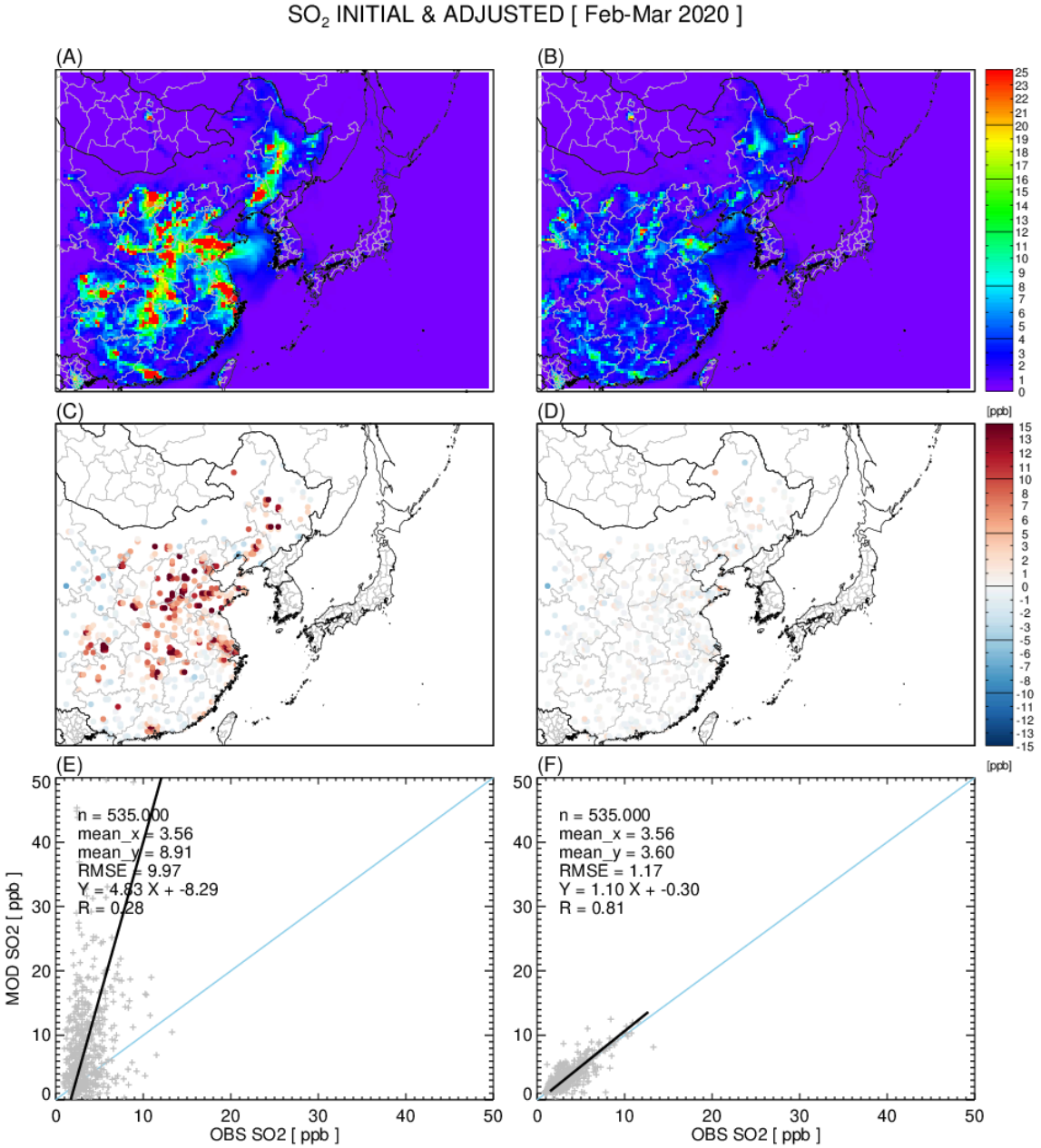

80 **Figure S8 Performance evaluation of models run with initial emissions inventory (A,C, E) and adjusted emissions (B, D, F) for SO_2, Feb-Mar 2020. Shown are spatial distributions of simulated SO_2 concentrations (top: A, B) and biases (middle: C, D), as well as scatter plot comparisons for initial (E) and adjusted (F) emissions for February to March 2020. Adjusted simulation is based on the 2-step method outlined in Section 3.2 of the main body of the paper.**

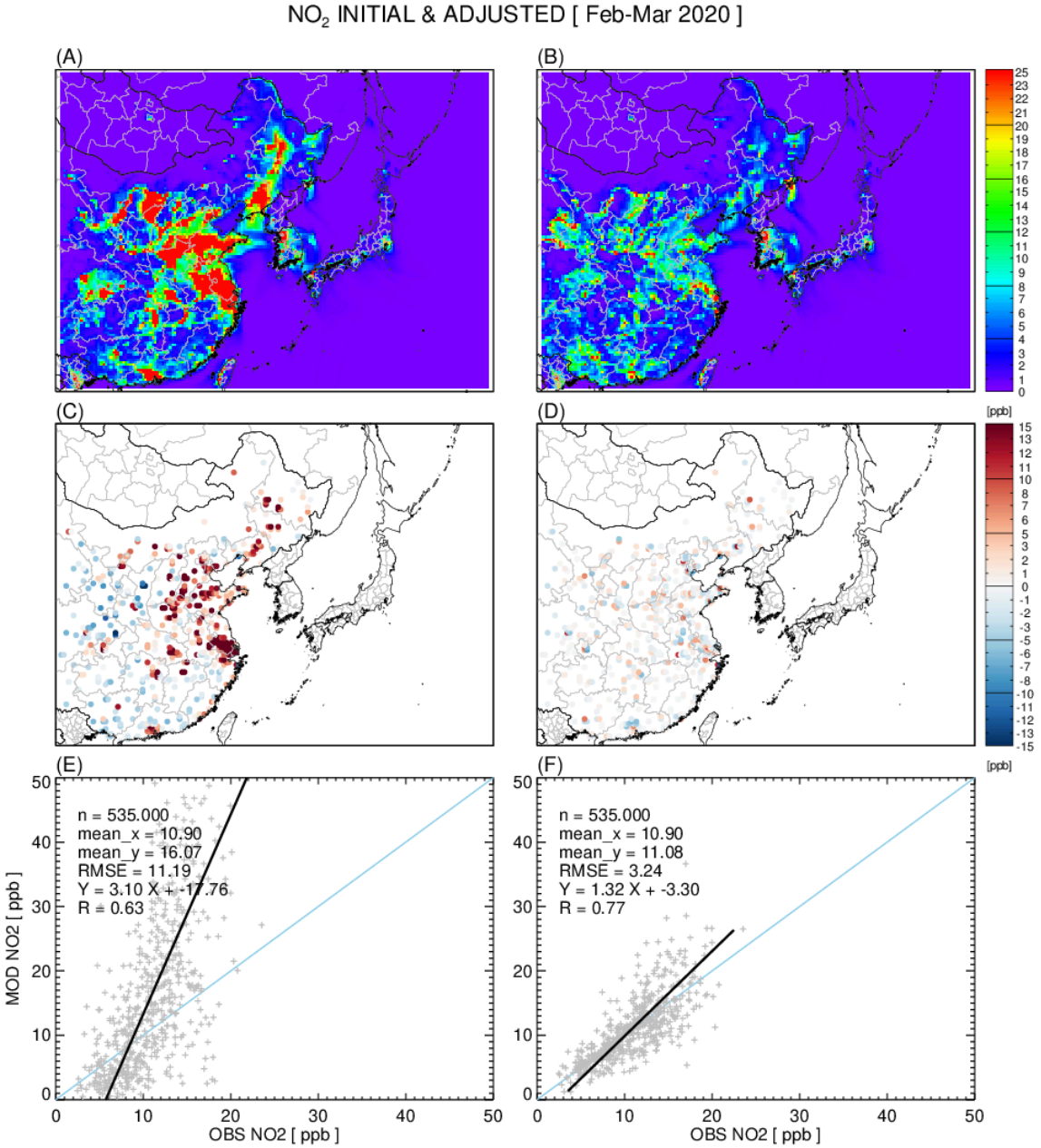

85

Figure S9 Performance evaluation of models run with initial emissions inventory (A,C, E) and adjusted emissions (B, D, F) for NO_2, Feb-Mar 2020. Shown are spatial distributions of simulated NO_2 concentrations (top: A, B) and biases (middle: C, D), as well as scatter plot comparisons for initial (E) and adjusted (F) emissions for February to March 2020. The adjusted simulation is based on the 2-step method outlined in Section 3.2 of the main body of the paper.

90

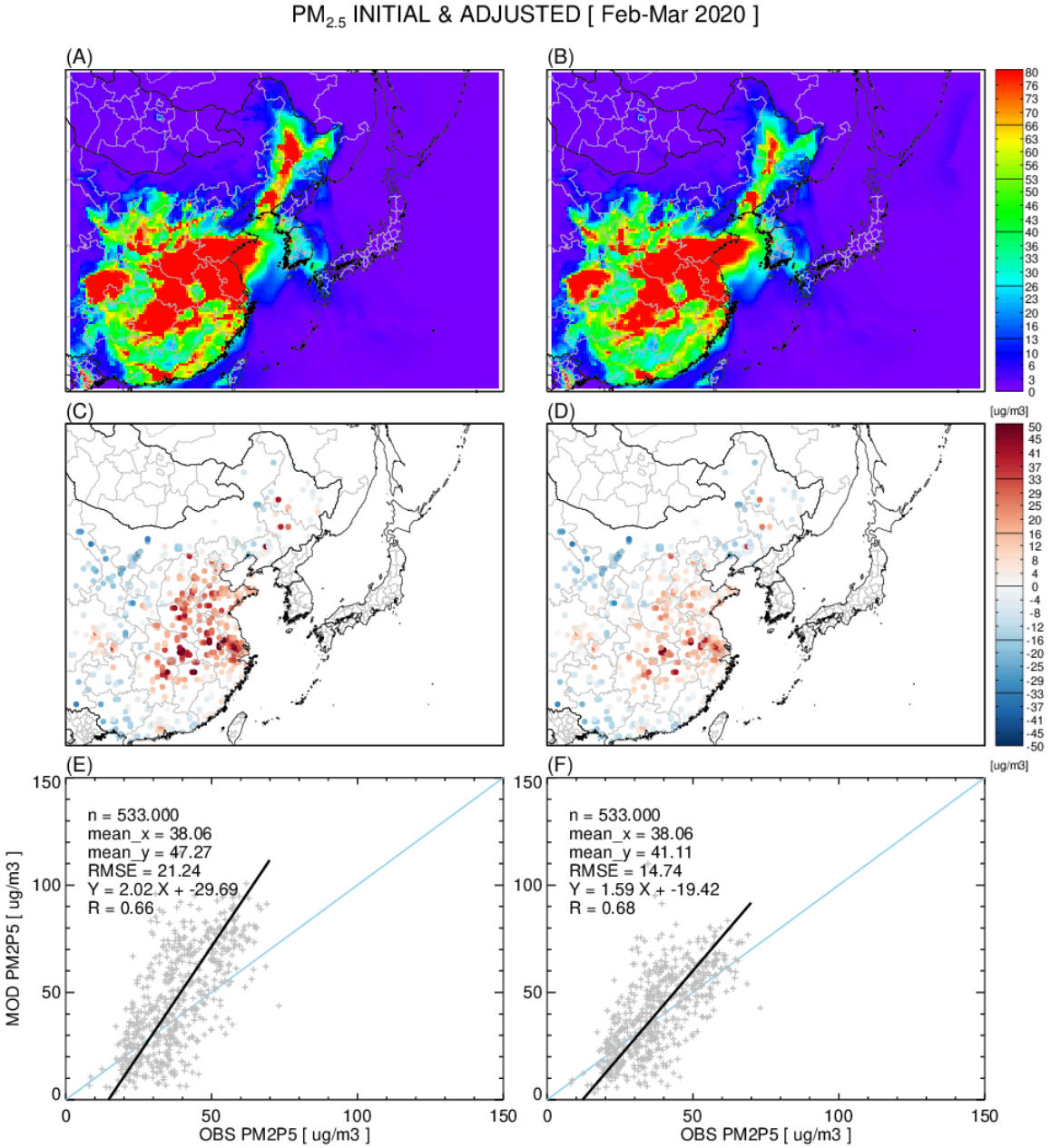

Figure S10 Performance evaluation of models run with initial emissions inventory (A,C, E) and adjusted emissions (B, D, F) for $PM_{2.5}$, Feb-Mar 2020. Also shown are spatial distributions of simulated $PM_{2.5}$ concentrations (top: A, B) and biases (middle: C, D), as well as scatter plot comparisons for initial (E) and adjusted (F) emissions for February to March 2020. The adjusted simulation is based on the 2-step method outlined in Section 3.2 of the main body of the paper.

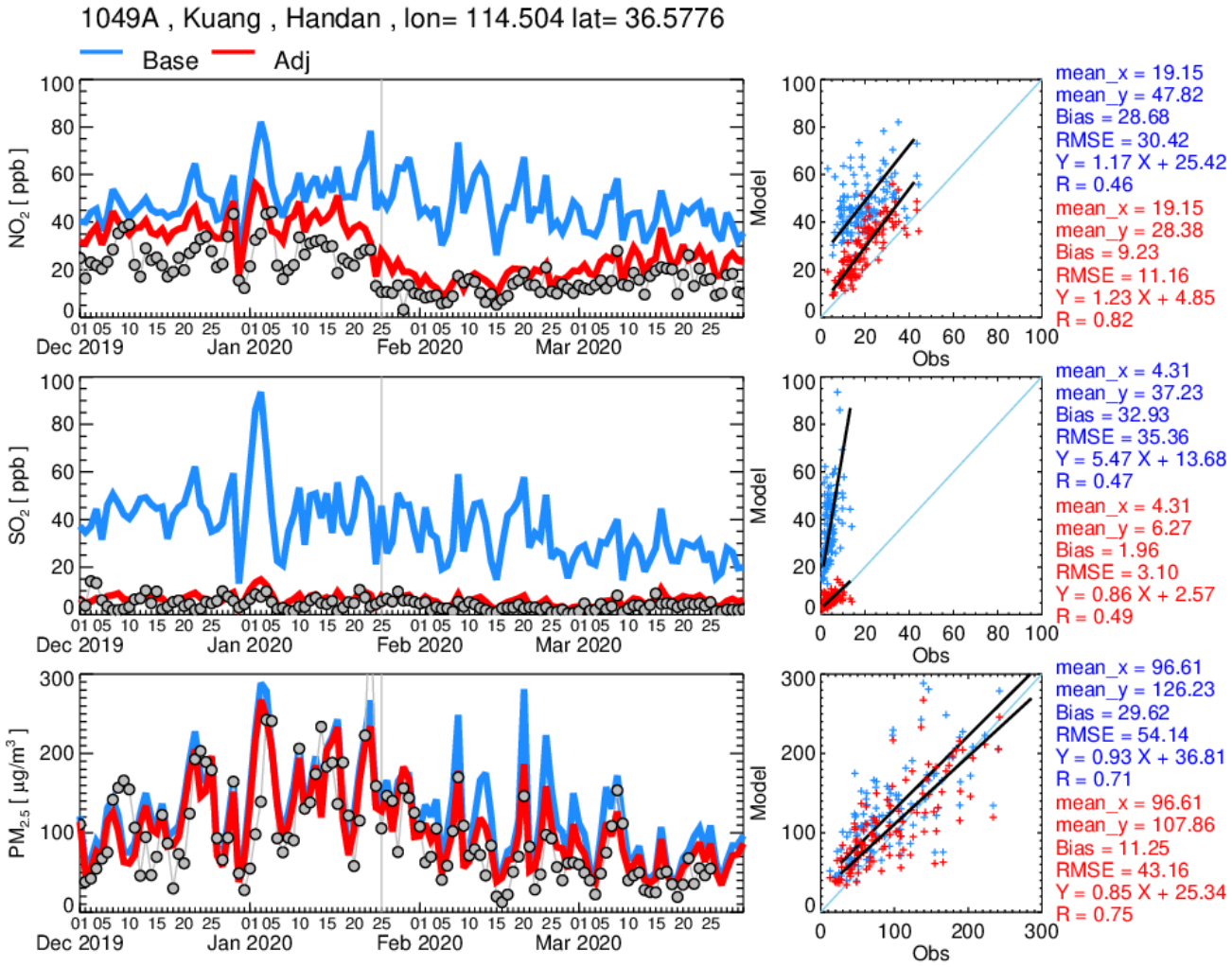

Figure S11 Time series and scatter plots of observed and modeled surface concentrations of SO_2, NO_2, and $PM_{2.5}$ from the Kuang, Handan monitoring site (lon=114.504, lat=36.5776, id=1049A). A further 1,570 plots are available at an external link (https://www.dropbox.com/s/e8czqza66jpcxz1/out-ts-all.tgz?dl=0).

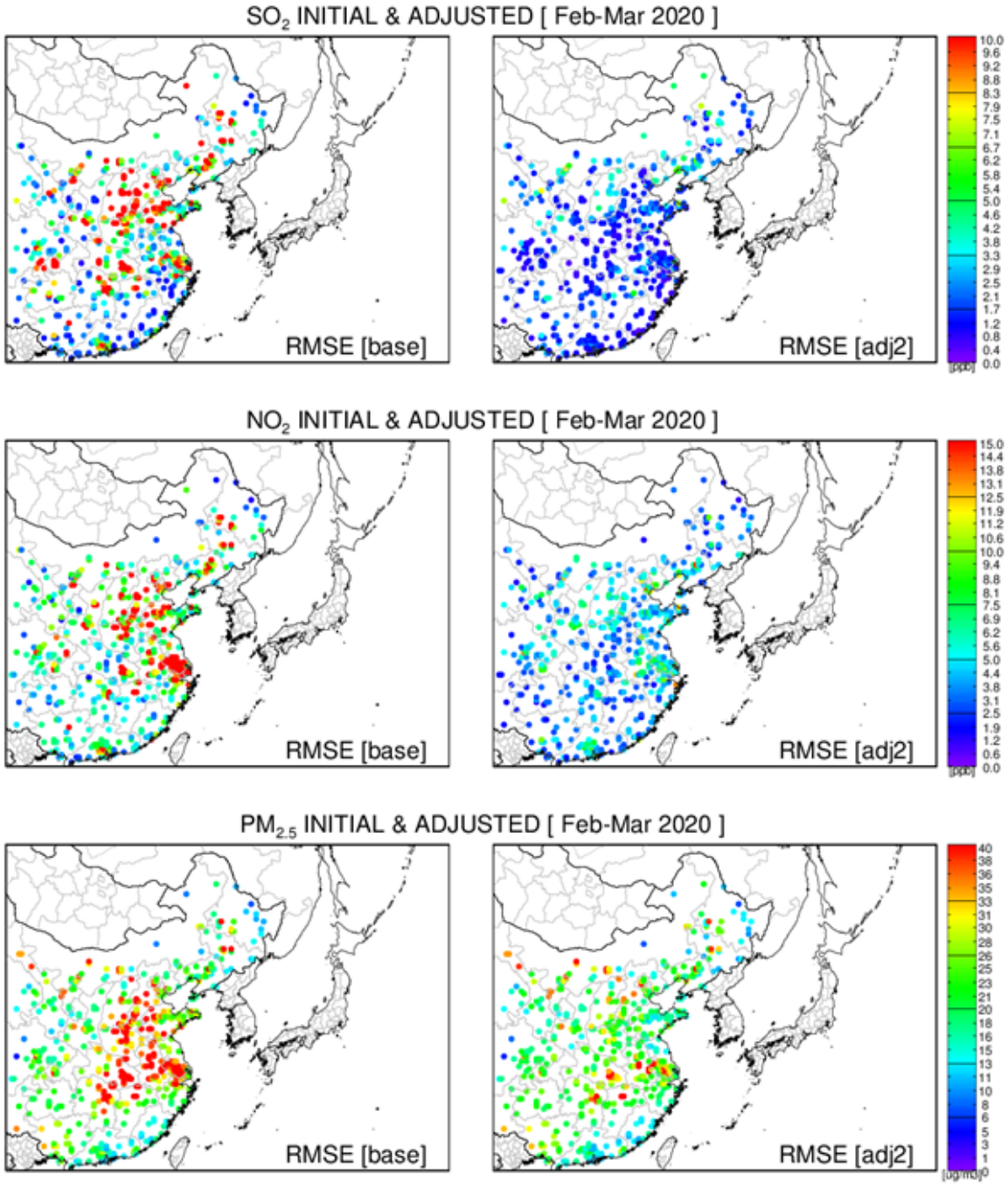

Figure S12 Spatial distributions RMSE for the base (left) and the adj2 run (right). RMSEs were calculated from daily mean concentrations during February and March 2020 for each monitor.

105

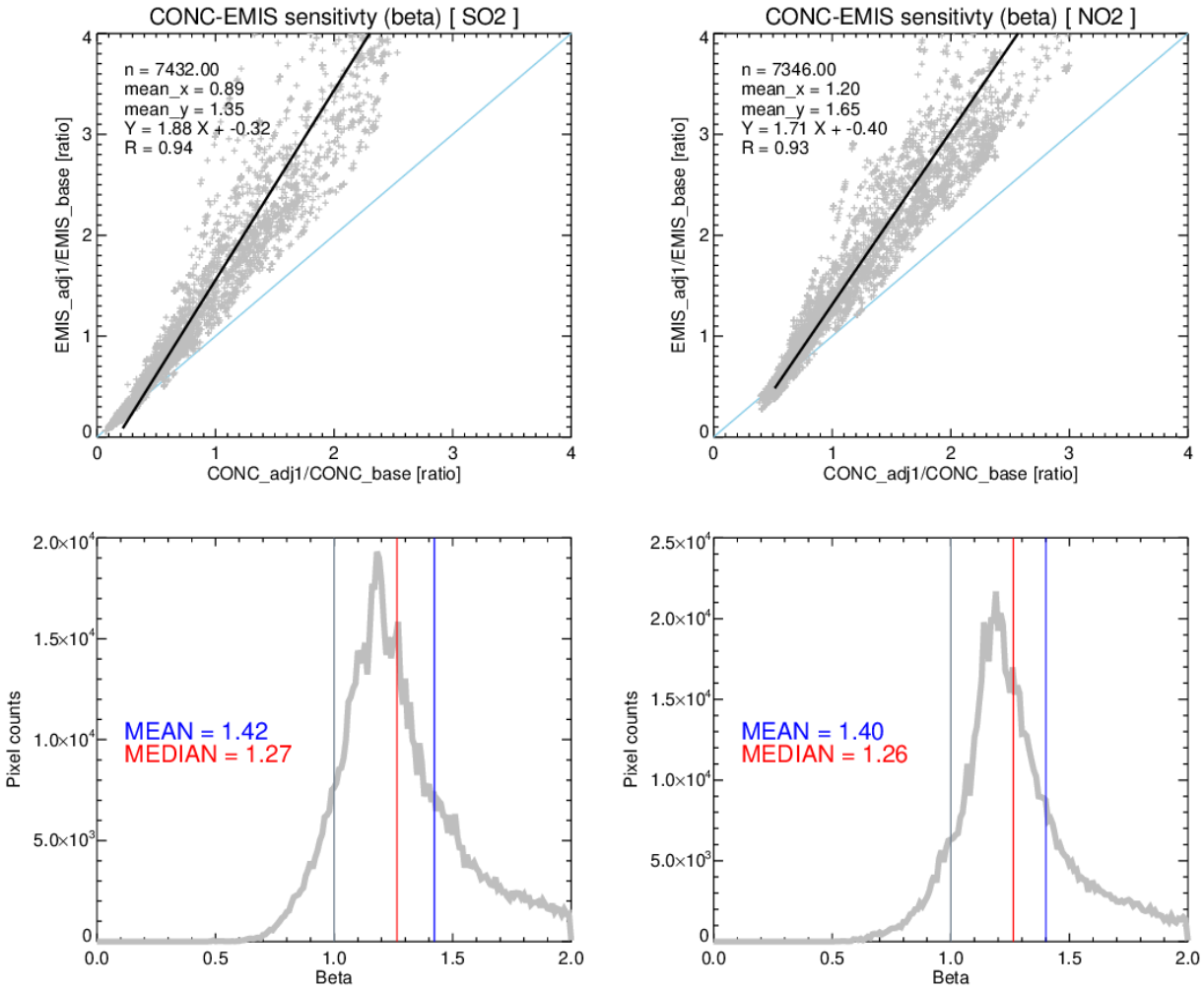

Figure S13 Calculation of the concentration-to-emissions sensitivities (β) for the emissions adjustment experiment of SO_2 and NO_2. The β values are obtained as the ratio of the emissions change (i.e. *Emis_adj*/*Emis_base*) to the change in concentrations (i.e. *Conc_adj1*/*Conc_base*), which is also consistent with the slope in the scatterplot (upper). The occurrences of the calculated β values for each domain pixel and daily timescale are summarized as the histogram plots (lower).